

Harnessing Desert Flora: Biogenic Silver Nanoparticles from Desert Plants Combat Bacterial Infections and Biofilm Formation

Mamona Nazir¹✉, Rabbia Ahmad¹, Muhammad Ehsan Mazhar², Muhammad Saleem³, Afifa Nazish¹, Shehla Perveen¹, Muniba Shafique¹, Asma Yaqoob⁴, Syed Adnan Ali Shah^{5,6}

¹ Department of Chemistry, Government Sadiq College Women University Bahawalpur, 63100-Bahawalpur, Pakistan

² Department of Physics, Bahauddin Zakariya University Multan, Multan 60800, Pakistan

³ Institute of Chemistry, Baghdad Campus, The Islamia University of Bahawalpur, Bahawalpur 63100, Pakistan

⁴ Department of Biochemistry, Institute of BBBI, The Islamia University of Bahawalpur, Bahawalpur 63100, Pakistan

⁵ Faculty of Pharmacy, Universiti Teknologi MARA Cawangan Selangor Kampus Puncak Alam, Bandar Puncak Alam 42300, Selangor Malaysia

⁶ Atta-ur-Rahman Institute for Natural Product Discovery (AuRIns), Universiti Teknologi MARA Cawangan Selangor Kampus Puncak Alam, Bandar Puncak Alam 42300, Selangor Malaysia

✉ Corresponding author. E-mail: mamonanazir.de@gscwu.edu.pk

Received: Jul. 29, 2023; **Revised:** Oct. 23, 2023; **Accepted:** Nov. 21, 2023

Citation: M. Nazir, R. Ahmad, M.E. Mazhar, et al. Harnessing desert flora: biogenic silver nanoparticles from desert plants combat bacterial infections and biofilm formation. *Nano Biomedicine and Engineering*, 2024, 16(2): 248–257.

<http://doi.org/10.26599/NBE.2024.9290058>

Abstract

In this study, we harnessed the properties of desert plants to synthesize silver nanoparticles to explore potential antimicrobial solutions. *Chrozophora plicata* and *Heliotropium curassavicum* extracts were used as green reducing agents to transform silver ions into nanoparticles. Our findings revealed novel properties of *C. plicata*, which have not been reported before. Surface plasmon resonance peak at 453.6 and 431 nm for *C. plicata* and *H. curassavicum*, respectively, via ultraviolet (UV) spectral analysis evidenced the successful fabrication of silver nanoparticles with particle sizes ranging from 4.3–8 and 3.1–6.97 nm respectively, which was validated by field emission scanning electron microscopy (FE-SEM). X-ray diffraction analysis revealed that the crystal structure of these nanoparticles had a face-centered cubic geometry. Fourier transform infrared spectrometry of the plant extract showed strong signals corresponding to carbohydrates, proteins, and phenolics. Antibacterial assays of the silver nanoparticles from *C. plicata* displayed zones of inhibition at 5 and 4 mm against *Staphylococcus aureus* and *Escherichia coli*, respectively. Meanwhile, the silver nanoparticles from *H. curassavicum* exhibited zones of inhibition against both pathogens at 10 and 7 mm, respectively. The test samples were substantial inhibitors of *S. aureus* and *E. coli* biofilm formation since these displayed IC₅₀ values in the range of 8.88–10.57 mg/mL, which is as potent as the reference ciprofloxacin. Consequently, the silver nanoparticles derived from these desert plants can be potential drug candidates for treating respiratory and digestive tract infections alone or in combination with existing antibiotics.

Keywords: biogenic synthesis; silver nanoparticles fabrication; desert plants extract; antimicrobial activity; biofilm inhibition; nanotechnology; antibiotic resistance.

Introduction

Nanotechnology is an emerging field that comprises nanoparticles of remarkable abilities due to their large surface area to volume ratio, unique catalytic activity, and recently discovered electronic, optic, and magnetic properties. Therefore, these nanoparticles have potential applications in numerous fields like biomedicine, pharmacology, nanobiotechnology, agriculture, manufacturing and materials, environment, electronics, energy collection, and mechanical industries [1–3]. Although physical and chemical methods have been extensively used to synthesize metal nanoparticles, they are usually labor-intensive, expensive, and produce hazardous byproducts that can damage the environment and living organisms [4–7]. Green synthetic methods utilizing microorganisms and plants (or their extracts) are currently being explored. Plant extracts contain diverse phytochemicals, including enzymes, polysaccharides, proteins, ascorbic acid, terpenoids, flavonoids, phenolics, sterols, alcohols, alkaloids, amines, and saponins [8, 9] that act as reducing agents to impart nanoparticles with diverse structural and morphological features [10, 11].

Among several noble metal nanoparticles, silver nanoparticles (AgNPs) are an arch product because their inter-band transition energy is placed away from the surface plasmon resonance energy [12, 13]. AgNPs possess various properties, such as antibacterial, antifungal, antiviral, antioxidant, and anticancer. They also act as excellent catalysts in degrading dyes, treating diabetes-related complications, and wound healing [14–17]. Recently, AgNPs have been used to improve the efficiency of antibiotics by damaging the microbial DNA [18]. Due to their antimicrobial properties, silver nanoparticles are also used in the production, storage, packaging, and transportation of food products and other kitchenware [19]. In agriculture, AgNPs act as larvicidal agents, nano-fertilizers, and nano-pesticides [20, 21]. Studies revealed that AgNPs are more potent than the plant extracts used for their preparation. For example, silver nanoparticles synthesized using the bark extracts of *Piceaabies* and *Pinusnigra* exhibit more potent antifungal, antibacterial, and antimetabolic properties than the bark extracts themselves [22]. Similarly, AgNPs synthesized using five different aqueous plant extracts, including *Berberis vulgaris*, *Brassica nigra*, *Capsella bursa-pastoris*, *Lavandula*

angustifolia, and *Origanum vulgare*, had improved size and morphology and exhibited enhanced antimicrobial activity [23]. Researchers also demonstrated that plant extracts used to prepare stable AgNPs only reduce and stabilize these AgNPs and thus can modulate immune and cytotoxic responses [24].

Chrozophora plicata (CP) is a medicinal plant growing in the Cholistan Desert near Bahawalpur, Pakistan. Based on chemical analysis, *C. plicata* leaves have been shown to contain triterpenoids, sterols, alcohols, hydrocarbons, and phenolics like flavonoids, lignans, coumarins, tannins, phenanthrenes, quinones, and phenolic acids [25]. Phytochemical screening of *C. plicata* indicates the presence of flavonoids, alkaloids (plicatanins A–C, speranberculatine A), coumarins (bilactone plicatanone, methyl p-coumarate), sterols (β -sitosterol), α -glucosidase (β -sitosterol-3-O- β -D-glucopyranoside, apigenin-5-O- β -D-glucopyranoside) [26, 27]. *Heliotropium curassavicum* (HC) is another plant found in the Cholistan Desert that contains many bioactive components, including pyrrolizidine alkaloids, flavonoids, terpenoids, other alkaloids, tannins, phenols, proteins, and steroids [28, 29]. Considering the diversity of the secondary metabolites in *C. plicate* and HC, we utilized these aqueous plant extracts to prepare AgNPs, which were then characterized using several analytical techniques in this study. We also evaluated their antibacterial and anti-biofilm formation potential.

Experimental

Preparation of plant extract

Whole *C. plicata* and *H. curassavicum* plants were collected during the flowering season (i.e., May 2022) from the fields around Civil Hospital, Bahawalpur. They were identified by Dr. Farrukh Nisar, a plant taxonomist in the Department of Biochemistry, Cholistan University of Veterinary and Animal Sciences, Bahawalpur, Pakistan. The plant specimens were cleaned with tap water several times to remove impurities and dust particles, washed with double distilled water, and dried under shade for 15 days. The dried material was chopped into small pieces. The plant extracts were prepared using deionized water, using a 1:10 (mL) volume ratio of plant material to water, followed by heating at 75 °C

for 90 min [30].

Synthesis of the AgNPs

Silver nitrate was obtained from Aldrich Chemical Co. (St. Louis, MO, USA) and was used without purification. Silver nitrate (0.09 g) was dissolved in deionized water (100 mL) and heated at 70 °C. Then, it was added dropwise into a filtered transparent aqueous solution of the plant extract (250 mL) under vigorous stirring for 20 min. The solution was stirred vigorously at 80 °C for 3 h until the color of the reaction mixture changed to dark brown and then allowed to cool to room temperature. This color change indicated the formation of AgNPs, which were purified using ultracentrifugation (2 h at 45 000 r/min) and then re-dispersed in water [31]. The AgNPs synthesized from *C. plicata* and *H. curassavicum* were named CP-AgNPs and HC-AgNPs, respectively.

Characterization of AgNPs

The AgNPs were characterized using ultraviolet–visible (UV–Vis) absorption spectroscopy with the Cary 60 UV–Vis spectrometer to confirm the reduction process. X-ray diffraction (XRD) analysis was performed using the EQUINOX 3000 XRD instrument (Thermo Scientific, France). The Fourier transform infrared (FTIR) spectra of the samples were acquired using the Agilent FTIR Cary-630 ATR with a KBr disk, ranging from 4 000 to 400 cm^{-1} . A TESCAN MAIA3 field emission scanning electron microscope (FE-SEM) equipped with an Octane Elite EDAX detector was employed to perform FE-SEM and energy-dispersive X-ray (EDX) studies on the prepared samples.

Bioactivity assays

Disc diffusion antibacterial assay

The samples of the synthesized AgNPs were tested against Gram-positive and Gram-negative bacteria (*Staphylococcus aureus* and *Escherichia coli*, respectively). These strains were cultured for 24 h at 37 °C on nutrient agar (Oxoid, UK). The disc diffusion method was used to determine the antibacterial activity of the test samples. After culturing the bacteria on a nutrient agar medium, 100 μL of culture suspension containing 10^7 colony-forming units (CFUs)/mL was used to measure the antibacterial activity of the NPs. Sterilized filter paper discs (6 mm in diameter) were independently soaked

in the sample solution and then placed on the agar plates inoculated with the test microorganisms. Empty discs and discs containing ciprofloxacin (30 $\mu\text{g}/\text{disc}$) (Oxoid, UK) were used as the negative control and reference, respectively. The plates were incubated for 2 h at 4 °C and then at 37 °C for 18 h. The diameters of the growth inhibition zone in mm (zone reader) were measured to evaluate the antibacterial activity of the organisms compared to the control [32, 33].

Biofilm inhibition assay

The biofilm formation inhibition assay was performed using a previously reported method [34, 35]. Sterile 96-well plates were filled with 100 μL of nutrient broth (Oxoid, UK) and 100 μL of test sample solution, followed by adding 20 μL of the bacterial culture suspension. Only nutrient broth was used as the negative control. The plates were covered and incubated aerobically at 37 °C for 24 h. Then, 220 μL of sterile phosphate buffer was used to wash the contents of each well thrice. The plates were shaken vigorously to remove all non-adherent bacteria. Then, 220 μL of 99% methanol was added per well to fix the remaining attached cells. After 15 minutes, the plates were dried and stained for 5 min with 220 μL of 50% crystal violet per well. After removing the excess stain using tap water, the plates were air dried, and 220 μL of 33% (v/v) glacial acetic acid per well was added to resolubilize the dye bound to the adherent cells. The optical density (OD) of each well was measured at 630 nm using a microplate reader (Bio Tek, USA). All the tests were performed in triplicates, and the averages were calculated. The bacterial growth inhibition (INH%) was calculated as follows:

$$\text{INH}\% = 100 - (\text{OD}_{630 \text{ sample}} * 100) / \text{OD}_{630 \text{ control}}$$

Results and Discussion

Characterization of the synthesized AgNPs

UV spectral analysis

The solid crystalline powder of AgNPs was dispersed in water to record the UV–Vis spectra. The synthesized CP- and HC-AgNPs exhibit surface plasmon resonance phenomenon at 453.6 and 431 nm, respectively (Fig. 1), as shown previously [36, 37], due to the combined vibration of the electrons in the

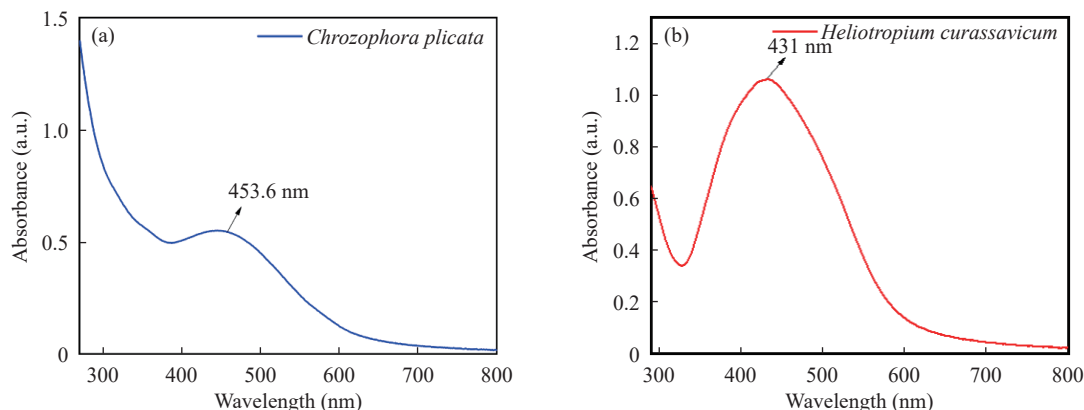


Fig. 1 UV-Vis spectra of AgNPs: (a) CP-AgNPs (b) HC-AgNPs.

AgNPs that resonate with light waves. Therefore, this preliminary data indicated the successful formation of stable CP- and HC-AgNPs.

XRD analysis

Using (XRD), we confirmed the phase changes and lattice structure of the prepared material. The interface of the incident rays with the test sample produces constructive interference and a diffracted ray when conditions satisfy Bragg’s Law ($n\lambda=2d \sin\theta$). The biosynthesized CP-AgNPs (Fig. 2(a)) showed XRD peaks at 2θ corresponding to $38.1^\circ(111)$, $44.3^\circ(200)$, and $64.4^\circ(220)$ (Table 1) of the face-centered cubic (FCC) silver [38] corresponding to the standard FCC structure, which was compared with JCPDS file No. 04-0783 from

previous studies [36]. The average crystalline size (D_c) of CP-AgNPs was estimated by using the following Debye–Scherrer equation:

$$D = K\lambda/(\beta\cos \theta)$$

where K is the Scherrer constant with a value of 0.9, λ is the wavelength of the X-ray, and usually, a Cu source with 0.59 nm wavelength is used as a source, β denotes the full width at half maximum, and the Bragg angle in radians is θ . The estimated crystalline size was observed to be 6.96 nm.

XRD at 2θ in the range of 35° – 80° was detected for the biosynthesized HC-AgNPs from three diffraction signals (planes) appearing at 38.17° , 46.37° , and 64.71° at 2θ , that matched with the (111), (200) and, (220) planes of FCC silver (JCPDS file No. 84-0713)

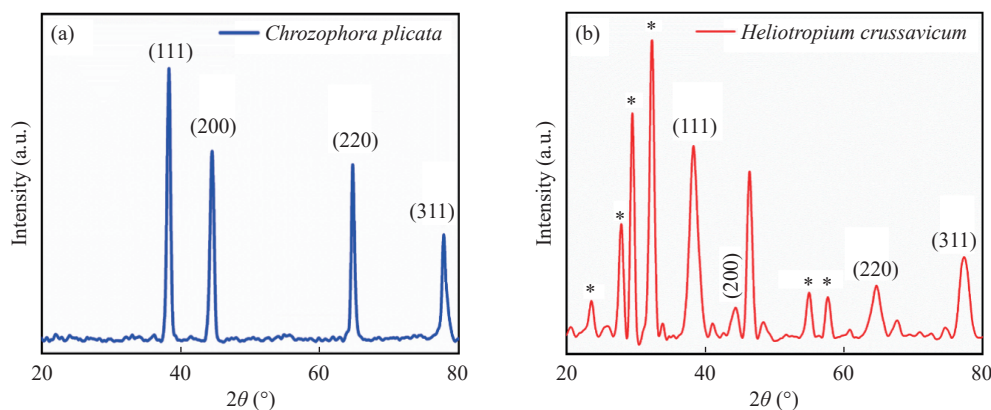


Fig. 2 XRD pattern of both the AgNPs: (a) CP-AgNPs and (b) HC-AgNPs.

Table 1 Calculated crystalline sizes of CP-AgNPs and HC-AgNPs

CP-AgNPs			HC-AgNPs		
2θ (°)	FWHM (rad)	Crystalline size (nm)	2θ (°)	FWHM (rad)	Crystalline size (nm)
38.1	0.466	18.85	38.17	11.88	0.74
44.3	9.784	0.92	46.37	0.60	15.05
64.4	8.85	1.11	64.71	11.88	0.83
Mean value		6.96	Mean value		5.54

(Fig. 2(b)). The unassigned peaks (marked with stars in Fig 2(b)) were also observed, indicating the crystallization of the bio-organic phase on the AgNP's surface [39]. Thus, the analyzed three signals of the HC-AgNPs proved that the HC-AgNPs were crystalline. The size of the HC-AgNPs crystals was calculated (as mentioned in Table 1) from all the signals collectively from Debye's equation. The mean size, calculated from all peaks, was 5.54 nm.

FTIR analysis

Fourier Transform infrared spectroscopy (FTIR) was used to analyze the molecules in the plant extracts involved in synthesizing the NPs (Fig. 3). The observed intense FTIR bands were compared with the previously reported standard values for identifying the functional groups. Figures 3(a) and 3(b) show the FTIR spectra of the CP- and HC-AgNPs, respectively. The broad absorption band at 3 247 cm^{-1} and 3 047 cm^{-1} (Fig. 3(a)) and 3 242 cm^{-1} and 3 050 cm^{-1} (Fig. 3(b)) corresponds to the O-H and C-H stretching vibration of phenols; it can be assumed that these phenolics are involved in the reduction of AgNO_3 to Ag^0 . The sharp band at 1 628 cm^{-1} (Fig. 3(a)) and 1 631 cm^{-1} (Fig. 3(b)) could be assigned to the C=O stretching of the lactone/ketone or carboxylic acid/anhydride group, respectively [40]. The dip at 1 402 cm^{-1} (Fig. 3(a)) is due to the N=O bending of the nitro group. The band observed at 1 112 cm^{-1} (Fig. 3(a)) represents the C–O stretching of esters [41, 42]. In the FTIR spectrum of HC-AgNPs (Fig. 3(b)), the band at 2 920 cm^{-1} was observed for aliphatic C-H stretching, whereas the band at 1461 cm^{-1} was due to the N=H stretching vibrations from various proteins. The peak at 1 272 cm^{-1} revealed the stretching of nitro compounds present in the extract. The dip at 1 272 cm^{-1} can be assigned to the C=N stretching vibration of amines [41, 43]. The bands

observed at 1 112 cm^{-1} (Fig. 3(a)) and 1 011 cm^{-1} (Fig. 3(b)) correspond to the C–O stretching vibrations [44]. This spectral information shows that the AgNPs must have been stabilized by the biomolecules. Since the phytochemicals in both plant extracts were screened and have also been reported in the literature, phenolic compounds, flavonoids, alkaloids, diterpenoids, and triterpenoids were found in significant quantities [45–47]. This substantiated the FTIR results and deduction of stabilizing the AgNPs primarily by phenolic compounds along with other metabolites.

FE-SEM analysis

The morphology and particle size of the biosynthesized AgNPs were evaluated using FE-SEM micrographs, while the particle size distribution was analyzed using the dynamic light scattering (DLS) histogram (Figs. 4 and 5). The results showed the presence of nano-spheres with diameters ranging from 4.3–8 and 3.1–6.97 nm for CP-AgNPs (Fig. 4) and HC-AgNPs (Fig. 5), respectively. This size range was consistent with the crystalline size calculated from Debye–Scherrer's equation. The presence of large particles can be related to slow reaction speed [48]. The synthesized AgNPs were uniformly distributed over a narrow diameter range in nm. The obtained NPs were also perfectly stabilized via the stabilizing and capping agents present in the plant extracts as validating using FTIR analysis.

EDX analysis

The energy dispersive X-Ray spectroscopy (EDX) analysis showed the successful synthesis of CP- and HC-AgNPs and estimated the elemental composition in percentages. The EDX profiles of the AgNPs displayed prominent peaks for elemental silver and small peaks for other elements (Fig. 6). The

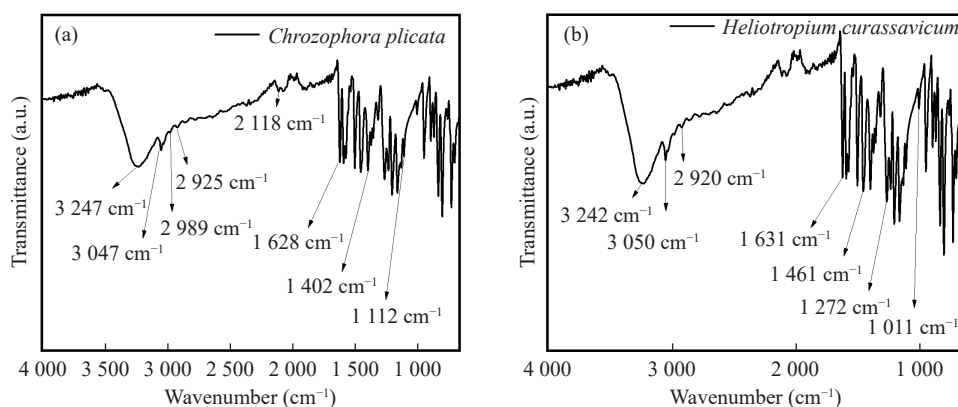


Fig. 3 FTIR spectra of the AgNPs; (a) CP-AgNPs (b) HC-AgNPs.

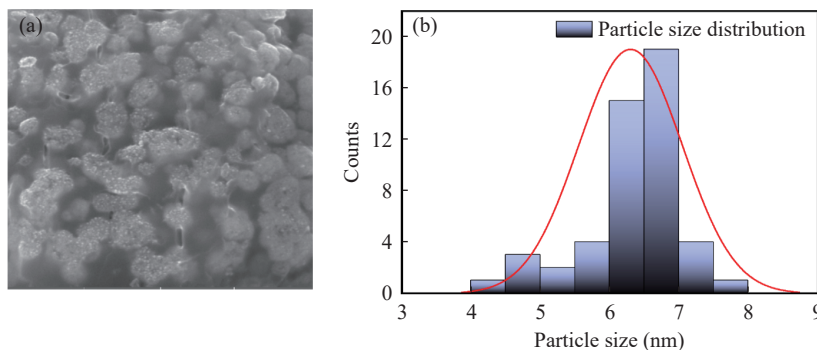


Fig. 4 (a) FE-SEM micrograph and (b) DLS histogram showing the particle size distribution of CP-AgNPs.

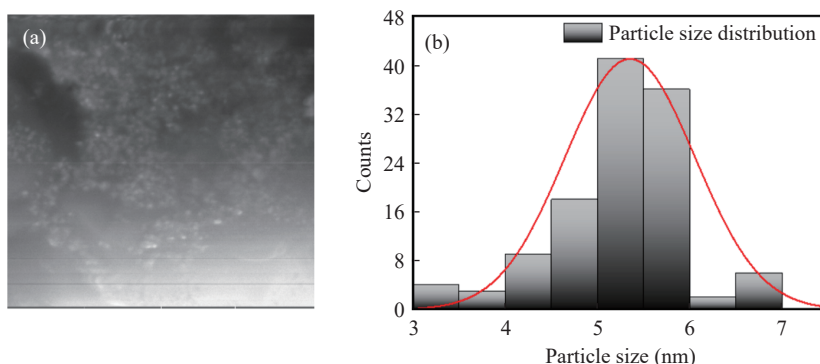


Fig. 5 (a) FE-SEM micrograph and (b) DLS histogram showing the particle size distribution of HC-AgNPs.

characteristic optical absorption peak at 3 keV is due to the surface plasmon resonance of the metallic silver nanocrystallites [49]. The elemental composition exhibited a high-intensity signal for Ag and weak signals for O, S, P, and Ca atoms. Moreover, the EDX analysis showed that the sample contained 51.05% and 4.29% (weight percentage) of silver biosynthesized from the *C. plicata* (Fig. 6(a)) and *H. curassavicum* (Fig. 6(b)) extracts, respectively. As shown previously, the low percentage of Ag in the HC-AgNPs can be attributed

to the nature of secondary metabolites in this plant, mostly pyrrolizidine alkaloids. This finding suggested that as phenolics are usually involved in the biosynthesis of AgNPs, higher concentrations of the *H. curassavicum* extract can enhance the percentage of Ag. Other signals observed for elemental Ag could be due to the biomolecules bound to the surface of AgNPs. The presence of S, P, and O peaks could be attributed to the cellular components, including carbohydrates, proteins, and other phytochemicals, which probably act as stabilizing or capping agents in synthesizing AgNPs [50]. These findings are consistent with the FTIR results, which showed the presence of functional groups involved in stabilizing the nanoparticles.

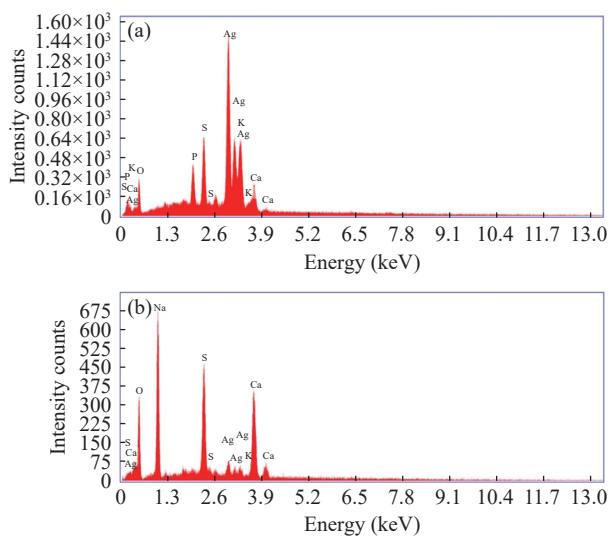


Fig. 6 EDX pattern (a) CP-AgNPs (b) HC-AgNPs.

Biological activities

Due to their morphological diversity, AgNPs exhibit various biological activities, making them useful for biomedical applications. In this study, the antibacterial and anti-biofilm formation activities of AgNPs synthesized using *C. plicata* (CP-AgNPs) and *H. curassavicum* (HC-AgNPs) extracts were evaluated.

The antibacterial assay results showed that the CP-AgNPs displayed moderate activity against *S. aureus* and *E. coli* (zones of inhibition or ZOI of 5 mm and 4 mm, respectively (Table 2)). Meanwhile, the HC-

Table 2 Antibacterial and anti-biofilm formation activities of CP-AgNPs and HC-AgNPs

Organism	Zone of inhibition (ZOI) (mm)			Biofilm formation inhibition IC ₅₀ (mg/mL)		
	CP-AgNPs	HC-AgNPs	Ciprofloxacin	CP-AgNPs	HC-AgNPs	Ciprofloxacin
<i>S. aureus</i>	5	10	27	10.16	10.57	8.33
<i>E. coli</i>	4	7	25	10.51	8.88	8.75

AgNPs exhibited significant activity against both pathogens, as the ZOI for *S. aureus* and *E. coli* were 10 and 7 mm, respectively (Table 2). Previous studies fully support our results, which showed that AgNPs synthesized from various sources showed similar antibacterial activities against *S. aureus* and *E. coli* [51]. Shahverdi *et al.* studied the synergic effect of AgNPs (reduced using *Klebsiella pneumoniae* culture supernatants) with different antibiotics against *S. aureus* and *E. coli*, which enhanced their activity [52].

Although they displayed moderate antibacterial activity, the potency of both CP- and HC-AgNPs in inhibiting biofilms formed by *S. aureus* (IC₅₀ = 10.16 and 10.57 mg/mL, respectively) and *E. coli* (IC₅₀ = 10.51 and 8.88 mg/mL, respectively) was similar to that of the standard drug ciprofloxacin (IC₅₀ = 8.33 and 8.75 mg/mL, respectively) (Table 2). Previous studies established that minor concentrations of AgNPs do not directly damage bacterial cells. This mechanism requires the dissolution of AgNPs to release sufficient silver ions to inhibit the biofilm formation by altering gene expression or inhibiting quorum sensing within the biofilm. The level of antibacterial activity of AgNPs has been shown to depend on their size, as smaller NPs show higher antimicrobial potential, probably because they can be easily internalized by bacterial cells [53].

Pathogenic bacteria form biofilms consisting of extracellular polysaccharides, DNA, and proteins for survival [54]. These biofilms protect the bacteria from various external stresses, including antibiotics, making these bacteria resistant to antibiotics. Therefore, inhibiting biofilm formation can prevent antimicrobial resistance [55], and biosynthesized AgNPs can be the best option to overcome this problem.

Conclusion

In this study, the aqueous extracts of *Chrozophora plicata* and *Heliotropium currasavicum* were used to

synthesize AgNPs with antibacterial and anti-biofilm forming properties. The synthesized materials were characterized by detecting the color change in the solution, UV-Vis and FTIR-spectroscopy, XRD, SEM, and EDX analysis. The particle sizes of CP-AgNPs and HC-Ag NPs ranged from 4.3–8 and 3.1–6.97 nm, respectively. The FTIR and UV-Vis spectra revealed that specific biomolecules, including phenolics, carbohydrates, and proteins, that are common in AgNPs might contribute to stabilizing AgNPs. The AgNPs synthesized from *C. plicata* (CP-AgNPs) exhibited ZOIs of 5 and 4 mm against *S. aureus* and *E. coli*, respectively, whereas AgNPs synthesized from *H. curassavicum* (HC-AgNPs) demonstrated ZOI against of 10 and 7 mm, respectively. Both test samples displayed IC₅₀ values ranging from 8.88–10.57 mg/mL, similar to the reference drug ciprofloxacin, indicating that they can significantly inhibit biofilm formation by *S. aureus* and *E. coli*. Hence, the AgNPs synthesized using the desert plants, *C. plicata* and *H. curassavicum*, might be potential candidates for developing future drugs to combat various bacterial infections.

CRedit Author Statement

The supervision of study, intellectual input, interpretation of data and first manuscript writing are credited to Mamona Nazir. Plant extracts were provided by Muhammad Saleem. Afifa Nazish performed synthesis of nano particles. Asma Yaqoob carried out antimicrobial and biofilm inhibition activities. Muhammad Ehsan Mazhar provided techniques for characterization. Shehla Perveen assisted in interpretation of data and manuscript writing. Rabbia Ahmad and Syed Adnan Ali Shah reviewed and edited the manuscript.

Acknowledgements

Authors acknowledge to Dr. Farrukh Nisar at Cholistan University of Veterinary and Animal

Sciences (CUVAS), Bahawalpur, Pakistan for identifying the plants material and Dr. Muhammad Farooq Warsi at Institute of Chemistry (IC), The Islamia University of Bahawalpur (IUB), Bahawalpur, Pakistan for his support for the synthesis of nanoparticles.

Conflict of Interests

The authors declare that there is no conflict of interest on financial or personal relationship for the reported work.

References

- [1] K.A. Khalil, H. Fouad, T. Elsamagawy, et al. Preparation and characterization of electrospun PLGA/silver composite nanofibers for biomedical applications. *International Journal of Electrochemical Science*, 2013, 8(3): 3483–3493. [https://doi.org/10.1016/s1452-3981\(23\)14406-3](https://doi.org/10.1016/s1452-3981(23)14406-3)
- [2] S.S. Salem, A. Fouda. Green synthesis of metallic nanoparticles and their prospective biotechnological applications: An overview. *Biological Trace Element Research*, 2021, 199(1): 344–370. <https://doi.org/10.1007/s12011-020-02138-3>
- [3] P.K. Dikshit, J. Kumar, A. Das, et al. Green synthesis of metallic nanoparticles: Applications and limitations. *Catalysts*, 2021, 11(8): 902. <https://doi.org/10.3390/catal11080902>
- [4] M.R., Das, R.K. Sarma, R. Saikia, et al. Synthesis of silver nanoparticles in an aqueous suspension of graphene oxide sheets and its antimicrobial activity. *Colloids and Surfaces B: Biointerfaces*, 2011, 83(1): 16–22. <https://doi.org/10.1016/j.colsurfb.2010.10.033>
- [5] K.-H. Cho, J.-E. Park, T. Osaka, et al. The study of antimicrobial activity and preservative effects of nanosilver ingredient. *Electrochimica Acta*, 2005, 51(5): 956–960. <https://doi.org/10.1016/j.electacta.2005.04.071>
- [6] Eid, M. Gamma radiation synthesis and characterization of starch based polyelectrolyte hydrogels loaded silver nanoparticles. *Journal of Inorganic and Organometallic Polymers and Materials*, 2011, 21(2): 297–305. <https://doi.org/10.1007/s10904-010-9448-4>
- [7] Srivastava, S. Biological nanofactories: Using living forms for metal nanoparticle synthesis. *Mini-Reviews in Medicinal Chemistry*, 2021, 21(2): 245–265. <https://doi.org/10.2174/18755607mtexentqo5>
- [8] M. Mohammadlou, H. Maghsoudi, H. Jafarizadeh-Malmiri. A review on green silver nanoparticles based on plants: Synthesis, potential applications and eco-friendly approach. *International Food Research Journal*, 2016, 23(2): 446–462.
- [9] P. Kuppusamy, M.M. Yusoff, G.P. Maniam, et al. Biosynthesis of metallic nanoparticles using plant derivatives and their new avenues in pharmacological applications - An updated report. *Saudi Pharmaceutical Journal*, 2016, 24(4): 473–484. <https://doi.org/10.1016/j.jsps.2014.11.013>
- [10] Sharma, D., Kanchi, S., Bisetty, K. Biogenic synthesis of nanoparticles: A review. *Arabian Journal of Chemistry*, 2019, 12(8): 3576–3600. <https://doi.org/10.1016/j.arabjc.2015.11.002>
- [11] E.-Y. Ahn, H. Jin, Y. Park. Assessing the antioxidant, cytotoxic, apoptotic and wound healing properties of silver nanoparticles green-synthesized by plant extracts. *Materials Science and Engineering: C*, 2019, 101: 204216. <https://doi.org/10.1016/j.msec.2019.03.095>
- [12] M. Ramya, M.S. Subapriya. Green synthesis of silver nanoparticles. *International Journal of Pharma Medicine and Biological Sciences*, 2012, 1: 54–61.(INVALID).
- [13] X.-F. Zhang, Z.-G. Liu, W. Shen, et al. Silver nanoparticles: Synthesis, characterization, properties, applications, and therapeutic approaches. *International Journal of Molecular Sciences*, 2016, 17(9): 1534. <https://doi.org/10.3390/ijms17091534>
- [14] S. Renganathan, S. Subramaniyan, N. Karunanithi, et al. Antibacterial, antifungal, and antioxidant activities of silver nanoparticles biosynthesized from bauhinia tomentosa Linn. *Antioxidants*, 2021, 10(12): 1959. <https://doi.org/10.3390/antiox10121959>
- [15] R. Rajkumar, G. Ezhumalai, M. Gnanadesigan. A green approach for the synthesis of silver nanoparticles by *Chlorella vulgaris* and its application in photocatalytic dye degradation activity. *Environmental Technology & Innovation*, 2021, 21: 101282. <https://doi.org/10.1016/j.eti.2020.101282>
- [16] L. Xu, Y.Y. Wang, J. Huang, et al. Silver nanoparticles: Synthesis, medical applications and biosafety. *Theranostics*, 2020, 10(20): 8996–9031. <https://doi.org/10.7150/thno.45413>
- [17] S.H. Hamed, E.A. Azooz, E.A.J. Al-Mulla. Nanoparticles-assisted wound healing: A review. *Nano Biomedicine and Engineering*, 2023, 15(4): 425–435. <https://doi.org/10.26599/nbe.2023.9290039>
- [18] F. Abdel-Wahab, N. El Menofy, A. El- Batal, et al. Enhanced antimicrobial activity of the combination of silver nanoparticles and different β Lactam antibiotics against methicillin resistant *Staphylococcus aureus* isolates. *Azhar International Journal of Pharmaceutical and Medical Sciences*, 2021, 1(1): 24–33. <https://doi.org/10.21608/aijpm.2021.53610.1017>
- [19] S. Ahmed, M. Ahmad, B.L. Swami, et al. A review on plants extract mediated synthesis of silver nanoparticles for antimicrobial applications: A green expertise. *Journal of Advanced Research*, 2016, 7(1): 17–28. <https://doi.org/10.1016/j.jare.2015.02.007>
- [20] K. Chandhirasekar, A. Thendralmanikandan, P. Thangavelu, et al. Plant-extract-assisted green synthesis and its larvicidal activities of silver nanoparticles using leaf extract of *Citrus medica*, *Tagetes lemmonii*, and *Tarrena asiatica*. *Materials Letters*, 2021, 287: 129265. <https://doi.org/10.1016/j.matlet.2020.129265>
- [21] D.K. Singh, S. Chatterjee, R.S. Purty. Titanium dioxide nanoparticles (nano-tio2) mitigate heavy metals stress in indian mustard (*Brassica juncea* L.) seedlings. *Plant Cell Biotechnology and Molecular biology*, 2021, 22(71-72): 131–140.
- [22] I. Macovei, S.V. Luca, K. Skalicka-Woźniak, et al. Phyto-functionalized silver nanoparticles derived from conifer bark extracts and evaluation of their antimicrobial and cytogenotoxic effects. *Molecules*, 2021, 27(1): 217. <https://doi.org/10.3390/molecules27010217>
- [23] A. Salayová, Z. Bedlovičová, N. Daneu, et al. Green synthesis of silver nanoparticles with antibacterial activity using various medicinal plant extracts: Morphology and antibacterial efficacy. *Nanomaterials*, 2021, 11(4): 1005. <https://doi.org/10.3390/nano11041005>
- [24] J. Mussin, V. Robles-Botero, R. Casañas-Pimentel, et al. Antimicrobial and cytotoxic activity of green synthesis silver nanoparticles targeting skin and soft tissue infectious agents. *Scientific Reports*, 2021, 11: 14566. <https://doi.org/10.1038/s41598-021-94012-y>

- [25] M.M.S.A. Alsiede, M.A. Abddrahman, A.E. Saeed. Total phenolic content, flavonoid concentration and antioxidant activity of *Chrozophora plicata* leaves and seeds extracts. *International Journal of Advanced Research*, 2015, 3(8): 986–993.
- [26] K.S. Kumar, A.S. Rao. Extraction, isolation and structural elucidation of flavonoid from *Chrozophora plicata* leaves and evaluation of its antioxidative potentials. *Asian Journal of Pharmaceutical and Clinical Research*, 2017, 10(4): 460. <https://doi.org/10.22159/ajpcr.2017.v10i4.17106>
- [27] A. Tabussum, N. Riaz, M. Saleen, et al. α -Glucosidase inhibitory constituents from *Chrozophora plicata*. *Phytochemistry Letters*, 2013, 6(4): 614–619. <https://doi.org/10.1016/j.phytol.2013.08.005>
- [28] M.K. Ghorri, M.A. Ghaffari, S.N. Hussain, et al. Ethnopharmacological, phytochemical and pharmacognostic potential of genus *heliotropium* L. *Turkish Journal of Pharmaceutical Sciences*, 2016, 13(2): 143–168. <https://doi.org/10.5505/tjps.2016.20591>
- [29] R. Suthar, H.A. Solanki. Phytochemical screening of halophytic plant *heliotropium curassavicum* L. *International Journal of Scientific Research in Science and Technology*, 2021: 141–145. <https://doi.org/10.32628/ijrst218221>
- [30] M.S. Mehata. Green route synthesis of silver nanoparticles using plants/ginger extracts with enhanced surface plasmon resonance and degradation of textile dye. *Materials Science and Engineering: B*, 2021, 273: 115418. <https://doi.org/10.1016/j.mseb.2021.115418>
- [31] F. Zamarchi, I.C. Vieira. Determination of paracetamol using a sensor based on green synthesis of silver nanoparticles in plant extract. *Journal of Pharmaceutical and Biomedical Analysis*, 2021, 196: 113912. <https://doi.org/10.1016/j.jpba.2021.113912>
- [32] D. Garibo, H.A. Borbón-Núñez, J.N.D. de León, et al. Green synthesis of silver nanoparticles using *Lysiloma acapulcensis* exhibit high-antimicrobial activity. *Scientific Reports*, 2020, 10: 12805. <https://doi.org/10.1038/s41598-020-69606-7>
- [33] M.E. Taghavizadeh Yazdi, J. Khara, M.R. Housaindokht, et al. Role of *Ribes khorassanicum* in the biosynthesis of AgNPs and their antibacterial properties. *IET Nanobiotechnology*, 2019, 13(2): 189–192. <https://doi.org/10.1049/iet-nbt.2018.5215>
- [34] I.A. Raheem, S.S. Hussain, R.H. Essa. The effect of new hydantoin derivative (compound) on *Acinetobacter baumannii* biofilm formation isolated from clinical sources. *Journal of University of Babylon for Pure and Applied Sciences*, 2018, 26(10): 71–79.
- [35] E. Elekhawy, W.A. Negm, M. El-Aasr, et al. Histological assessment, anti-quorum sensing, and anti-biofilm activities of *Dioon spinulosum* extract: in vitro and in vivo approach. *Scientific Reports*, 2022, 12: 180. <https://doi.org/10.1038/s41598-021-03953-x>
- [36] J. Umashankari, D. Inbakandan, T.T. Ajithkumar, et al. Mangrove plant, *Rhizophora mucronata* (Lamk, 1804) mediated one pot green synthesis of silver nanoparticles and its antibacterial activity against aquatic pathogens. *Aquatic Biosystems*, 2012, 8: 11. <https://doi.org/10.1186/2046-9063-8-11>
- [37] S. Saranya, K. Vijayarani, K. Ramya, et al. Synthesis and characterization of silver nanoparticles using *azadirachta indica* leaf extract and their Lanti-fungal activity against *Malassezia* species. *Journal of Nano Research*, 2016, 43: 1–10. <https://doi.org/10.4028/www.scientific.net/JNanoR.43.1>
- [38] N.E.A. El-Naggar, M.H. Hussein, El-Sawah, A.A. Bio-fabrication of silver nanoparticles by phycocyanin, characterization, *in vitro* anticancer activity against breast cancer cell line and *in vivo* cytotoxicity. *Scientific Reports*, 2017, 7: 10844. <https://doi.org/10.1038/s41598-017-11121-3>
- [39] M. Vanaja, G. Annadurai. *Coleus aromaticus* leaf extract mediated synthesis of silver nanoparticles and its bactericidal activity. *Applied Nanoscience*, 2013, 3(3): 217–223. <https://doi.org/10.1007/s13204-012-0121-9>
- [40] M. Goudarzi, N. Mir, M. Mousavi-Kamazani, et al. Biosynthesis and characterization of silver nanoparticles prepared from two novel natural precursors by facile thermal decomposition methods. *Scientific Reports*, 2016, 6: 32539. <https://doi.org/10.1038/srep32539>
- [41] K. Jyoti, M. Baunthiyal, A. Singh. Characterization of silver nanoparticles synthesized using *Urtica dioica* Linn. leaves and their synergistic effects with antibiotics. *Journal of Radiation Research and Applied Sciences*, 2016, 9(3): 217–227. <https://doi.org/10.1016/j.jrras.2015.10.002>
- [42] K. Paulkumar, G. Gnanajobitha, M. Vanaja, et al. Green synthesis of silver nanoparticle and silver based chitosan bionanocomposite using stem extract of *Saccharum officinarum* and assessment of its antibacterial activity. *Advances in Natural Sciences: Nanoscience and Nanotechnology*, 2017, 8(3): 035019. <https://doi.org/10.1088/2043-6254/aa7232>
- [43] S. Honary, H. Barabadi, E. Gharaei-Fathabad, et al. Green synthesis of silver nanoparticles induced by the fungus *penicillium citrinum*. *Tropical Journal of Pharmaceutical Research*, 2013, 12(1): 7–11. <https://doi.org/10.4314/tjpr.v12i1.2>
- [44] M.A. Huq. Green synthesis of silver nanoparticles using *pseudoduganella eburnea* MAHUQ-39 and their antimicrobial mechanisms investigation against drug resistant human pathogens. *International Journal of Molecular Sciences*, 2020, 21(4): 1510. <https://doi.org/10.3390/ijms21041510>
- [45] W.H. Jasim, M.N. Hamad. Extraction and identification of phenolic compounds from the Iraqi *Heliotropium europaeum* L. plant. *Iraqi Journal of Pharmaceutical Sciences*, 2021, 30(2): 158–166. <https://doi.org/10.31351/vol30iss2pp158-166>
- [46] C. Pothiraj, P. Balaji, R. Shanthi, et al. Evaluating antimicrobial activities of *Acanthus ilicifolius* L. and *Heliotropium curassavicum* L. against bacterial pathogens: an *in-vitro* study. *Journal of Infection and Public Health*, 2021, 14(12): 1927–1934. <https://doi.org/10.1016/j.jiph.2021.10.013>
- [47] N. Riaz, A. Tabussum, M. Saleem, et al. Bioactive Secondary Metabolites from *Chrozophora plicata*. *Journal of the Chemical Society of Pakistan*, 2014, 36(2): 296–304.
- [48] C. Jayaseelan, R. Ramkumar, A.A. Rahuman, et al. Green synthesis of gold nanoparticles using seed aqueous extract of *Abelmoschus esculentus* and its antifungal activity. *Industrial Crops and Products*, 2013, 45: 423–429. <https://doi.org/10.1016/j.indcrop.2012.12.019>
- [49] S. Phongtongpasuk, S. Poadang, N. Yongcanich. Environmental-friendly method for synthesis of silver nanoparticles from dragon fruit peel extract and their antibacterial activities. *Energy Procedia*, 2016, 89: 239–247. <https://doi.org/10.1016/j.egypro.2016.05.031>
- [50] R. Palani velana, P.M. Ayyasama, R. Kathiravanb, et al. Rapid decolorization of synthetic melanoidin by bacterial extract and their mediated silver nanoparticles as support. *Journal of Applied Biology & Biotechnology*, 2015, 3(2): 6–11. <https://doi.org/10.7324/JABB.2015.3202>
- [51] X.H. Vu, T.T.T. Duong, T.T.H. Pham, et al. Synthesis and study of silver nanoparticles for antibacterial activity against *Escherichia coli* and *Staphylococcus aureus*.

- Advances in Natural Sciences: Nanoscience and Nanotechnology*, 2018, 9(2): 025019. <https://doi.org/10.1088/2043-6254/aac58f>
- [52] A.R., Shahverdi, A. Faknimi, H.R. Shahverdi, et al. Synthesis and effect of silver nanoparticles on the antibacterial activity of different antibiotics against *Staphylococcus aureus* and *Escherichia coli*. *Nanomedicine: Nanotechnology, Biology and Medicine*, 2007, 3(2): 168–171. <https://doi.org/10.1016/j.nano.2007.02.001>
- [53] P. Singh, S. Pandit, C. Jers, et al. Silver nanoparticles produced from *Cedecea* sp. exhibit antibiofilm activity and remarkable stability. *Scientific Reports*, 2021, 11: 12619. <https://doi.org/10.1038/s41598-021-92006-4>
- [54] H.-C. Flemming, J. Wingender. Relevance of microbial extracellular polymeric substances (EPSs) - Part I: Structural and ecological aspects. *Water Science and Technology*, 2001, 43(6): 1–8. <https://doi.org/10.2166/wst.2001.0326>
- [55] A. Di Somma, A. Moretta, C. Canè, et al. Inhibition of bacterial biofilm formation. In: *Bacterial Biofilms*. IntechOpen, 2020. <https://doi.org/10.5772/intechopen.90614>

© The author(s) 2024. This is an open-access article distributed under the terms of the Creative Commons Attribution 4.0 International License (CC BY) (<http://creativecommons.org/licenses/by/4.0/>), which permits unrestricted use, distribution, and reproduction in any medium, provided the original author and source are credited.